AD-A125 500 SPECIAL FINITE ELEMENTS FOR SHEETS WITH LOADED CIRCULAR HOLES(U) AERONAUTICAL RESEARCH LABS MELBOURNE (AUSTRALIA) K C WATTERS JUN 82 ARL/STRUC-392 1/1

UNCLASSIFIED F/G 20/11 NL

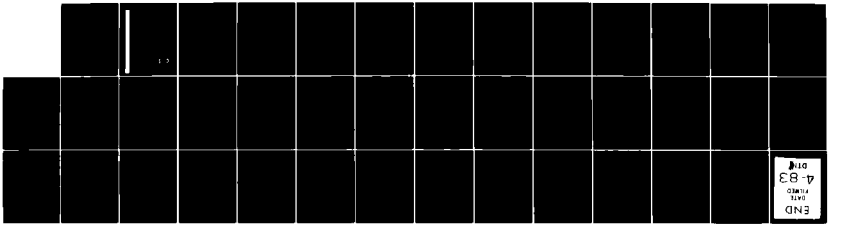

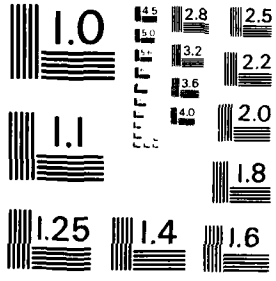

ARL-STRUC-REPORT-392

AR-002-895

DEPARTMENT OF DEFENCE SUPPORT

DEFENCE SCIENCE AND TECHNOLOGY ORGANISATION

AERONAUTICAL RESEARCH LABORATORIES

MELBOURNE, VICTORIA

STRUCTURES REPORT 392

SPECIAL FINITE ELEMENTS FOR SHEETS WITH LOADED CIRCULAR HOLES

by

K. C. WATTERS

Approved for Public Release

JUNE, 1982

COPY No

AR-002-895

DEPARTMENT OF DEFENCE SUPPORT
DEFENCE SCIENCE AND TECHNOLOGY ORGANISATION
AERONAUTICAL RESEARCH LABORATORIES

STRUCTURES REPORT 392

SPECIAL FINITE ELEMENTS FOR SHEETS WITH LOADED CIRCULAR HOLES

by

K. C. WATTERS

SUMMARY

This paper describes a special hybrid finite element to represent a loaded hole in a sheet. The shape functions of the element satisfy stress equilibrium and strain compatibility throughout the element, and the applied loading boundary conditions. The applied loading is represented by a finite Fourier series, and the coefficients of the element shape functions are matched with the Fourier coefficients. A computer program has been written to generate the element stiffness and stress recovery matrices. The program also produces equivalent nodal forces and initial stresses related to the applied loading. Accurate results have been obtained from several example analyses.

POSTAL ADDRESS: Chief Superintendent, Aeronautical Research Laboratories,
Box 4331, P.O., Melbourne, Victoria, 3001, Australia.

CONTENTS

NOTATION

a_n, b_n, c_n, d_n	Arbitrary stress function parameters at frequency n
b	Element thickness
C	Matrix relating nodal displacements to generalised parameters
D	Elasticity matrix
$\mathbf{d}$	Vector of displacements at any point in the element region
e_0, e_1, f_1	Arbitrary stress function parameters associated with special solutions of the bi-harmonic equation
f	The proportion of a full circle for the element variant shape
G	Element stiffness matrix in terms of generalised parameters
H	Matrix relating strains to generalised parameters
K	Element stiffness matrix in global cartesian co-ordinates
k	Element stiffness matrix in local polar co-ordinates
L	Matrix relating displacements to generalised parameters
N	Number of nodes
N_S	Cutoff frequency for the Fourier representation of the applied loading
n	General frequency parameter
$\mathbf{p}$	Vector of applied loads
p_0	Internal pressure
$\mathbf{Q}$	Vector of nodal loads in global carteisan co-ordinates
$\mathbf{q}$	Vector of nodal loads in local polar co-ordinates
r_0	radius of hole
r_1	Circumscribing radius of the element
r_{EQ}	Equivalent radius of the element
r, θ	Radial and angular co-ordinates of the local polar system
S	Stress recovery matrix
s_{1n}, s_{2n}	Stress function coefficients at frequency n related to the applied loading
T	A geometric transformation matrix
u, v	Radial and tangential displacements in the polar co-ordinate system
$\boldsymbol{\alpha}$	Vector of arbitrary generalised parameters
$\boldsymbol{\alpha}_0$	Vector of generalised parameters related to the applied loading
β_1, β_2, β_3	Rigid body motion parameters for x and y translation and rotation respectively
γ_i	Angular co-ordinate of node i

$\boldsymbol{\delta}$	Vector of nodal point displacements in local polar co-ordinates
$\boldsymbol{\Delta}$	Vector of nodal point displacements in global cartesian co-ordinates
$\boldsymbol{\epsilon}$	Vector of strain components
$\boldsymbol{\sigma}$	Vector of stress components
σ_{rr}, $\sigma_{\theta\theta}$, $\tau_{r\theta}$	Radial, tangential and shear stress components
$\sigma_a(\theta)$, $\tau_a(\theta)$	Distributions of normal and shear applied loading
σ_{ai}, τ_{ai}	Fourier coefficients of applied loading
ϕ	General symbol for a stress function
ν	Poisson's ratio

Subscripts

0	Refers to quantities related to the applied loading
H	Refers to quantities related to an unloaded hole
T	Refers to the full stress reco ery matrix constructed from evaluations at selected points
n	Refers to frequency n
Numerical	Refers to frequency or node number

Superscripts

T	Transpose
-1	Inverse
$'$	Dash superscript indicates quantities related to the orthogonal trigonometric functions to those of the undashed quantities
*	Arbitrary imposed state

1. INTRODUCTION

In this paper, a special finite element enclosing a loaded hole in a plane sheet is described in some detail. This work had its origins in an attempt to develop a special element to enclose a fragment damage site in an aircraft structure; such an element would facilitate residual strength analyses of damaged aircraft structures for use in vulnerability assessments. For example, when an aircraft is attacked by certain types of warhead the damage incurred by the aircraft skin consists of many closely spaced fragment perforations which can be idealised as holes with cracks radiating from them. A natural first step was to consider the case where the damage consists of uncracked circular holes in a plane sheet. Since problems involving sheets with circular holes, both unloaded and loaded, are of common occurrence in aircraft structures, quite apart from the particular application which gave rise to the present study, these were considered in detail; see also Reference 1.

The basic concept of the finite element method of structural analysis is that a complex structure is partitioned into a network of simple shaped, standard elements. The stiffness characteristic of the whole structure is then formed by assembling the known stiffness characteristics of the individual elements; see Reference 2. However, for regions of high stress gradients, such as occur around holes, it has proved beneficial to develop special element types, rather than to use fine meshes of standard elements. Rao *et al.*[3,4] were among the earliest to apply this concept. In Reference 3, a general method for formulating special elements around stress concentrators, including stress singularities, is presented. For this method, the displacement state within the element is defined by functions which satisfy conditions of stress equilibrium, strain compatibility, and any boundary conditions (BCs) of the stress concentrator. Such elements are termed "hybrid elements" in Reference 3, in that they combine concepts of continuum mechanics with finite elements. A consequence of the use of rather complex displacement functions for hybrid elements is that boundary displacements are incompatible with those of adjoining standard elements. However, a comparison[4] of two sector elements, one with "natural mode" shape (i.e. displacement) functions and the other with simple conforming shape functions, has clearly demonstrated the superior performance of the former despite its violation of inter-element displacement compatibility.

In Reference 3, Rao *et al.* demonstrate the use of a special hybrid element surrounding an unloaded circular hole in plane stress problems. In the present paper that work is extended to the case of loaded circular holes. The paper is set out as follows. A general outline of hybrid element theory is given in Section 2. Then, in Section 3, the detailed application of that theory to derive an element for a loaded circular hole is given, and in Section 4, the associated computer program is full described. Results of sample runs of the program are presented in Section 5, and a general discussion is given in Section 6.

2. HYBRID ELEMENT THEORY

For the stress analysis of two-dimensional elastic structures, the governing equation of equilibrium and compatibility is:[5]

$$\nabla^4 \phi = 0 \tag{2.1}$$

where ϕ is the stress function and ∇ is a differential operator, defined in polar co-ordinates by:

$$\nabla^2 = \frac{\partial^2}{\partial r^2} + \frac{1}{r}\frac{\partial}{\partial r} + \frac{1}{r^2}\frac{\partial^2}{\partial \theta^2} \tag{2.2}$$

A separated variable solution is proposed for ϕ in the form:

$$\phi = F(r)G(\theta) \tag{2.3}$$

where

$$G(\theta) = \begin{Bmatrix} \sin n\theta \\ \cos n\theta \end{Bmatrix}. \tag{2.4}$$

The upper and lower functions in the bracketed notation are each separately valid. On solving (2.1), (2.3) becomes:

$$\phi_n = [a_n r^n + b_n r^{-n} + c_n r^{2-n} + d_n r^{2-n}] \begin{Bmatrix} \sin n\theta \\ \cos n\theta \end{Bmatrix} \tag{2.5}$$

with the two degenerate cases:

$$\phi_0 = a_0 + b_0 \ln r + c_0 r^2 + d_0 r^2 \ln r \tag{2.6}$$

$$\phi_1 = [a_1 r + b_1 r^{-1} + c_1 r^3 + d_1 \ln r] \begin{Bmatrix} \sin \theta \\ \cos \theta \end{Bmatrix}. \tag{2.7}$$

The general frequency parameter, n, is unrestricted at this stage. In Reference 5 are listed several other solutions to (2.1), not in the form of (2.4), which together with (2.5), (2.6) and (2.7), make up the full general solution to (2.1) in polar co-ordinates. These other solutions are grouped below as:

$$\phi_e = e_0 r^2\theta + f_0\theta + e_1 r\theta \begin{Bmatrix} -\cos \theta \\ \sin \theta \end{Bmatrix}. \tag{2.8}$$

Using standard formulae,[5] the stresses, strains and displacements can be derived from the stress function. Having derived these quantities, the boundary conditions of a stress concentrator can be satisfied. For example, an unloaded hole has the boundary conditions:

$$\sigma_{rr} = \tau_{r\theta} = 0 \qquad \text{at } r = r_0 \text{ all } \theta. \tag{2.9}$$

These conditions allow two of the arbitrary coefficients a_n, b_n, c_n and d_n to be determined in terms of the other two. The allowable values for n are restricted to integers only, to satisfy a requirement for single-valuedness in a multiply-connected region. Conditions of symmetry can further restrict the allowable values for n. Once these boundary, single-valuedness and symmetry conditions have been applied to the general solution to (2.1), a set of functions remains which satisfies equilibrium, compatibility, and all conditions of the stress concentrator. For the general case of this set of functions, the radial and tangential displacements take the respective forms:

$$u = [f_{11}(n, r_0, r)b_n + f_{12}d_n] \begin{Bmatrix} \sin n\theta \\ \cos n\theta \end{Bmatrix} \tag{2.10}$$

$$v = [f_{21}b_n + f_{22}d_n] \begin{Bmatrix} -\cos n\theta \\ \sin n\theta \end{Bmatrix}. \tag{2.11}$$

The equations can be grouped in matrix form as:

$$\mathbf{d}_n = \begin{Bmatrix} u \\ v \end{Bmatrix} = \begin{bmatrix} f_{11} \begin{Bmatrix} \sin n\theta \\ \cos n\theta \end{Bmatrix} & f_{12} \begin{Bmatrix} \sin n\theta \\ \cos n\theta \end{Bmatrix} \\ f_{21} \begin{Bmatrix} -\cos n\theta \\ \sin n\theta \end{Bmatrix} & f_{22} \begin{Bmatrix} -\cos n\theta \\ \sin n\theta \end{Bmatrix} \end{bmatrix} \begin{Bmatrix} b_n \\ d_n \end{Bmatrix} \tag{2.12}$$

i.e.

$$\mathbf{d}_n = L_n \boldsymbol{\alpha}_n \quad \text{(say)}. \tag{2.13}$$

When the functions for several values of n contribute to the displacement, it is given by:

$$\mathbf{d} = \Sigma \mathbf{d}_n = [L_i, L_j, L_k, \ldots] \begin{Bmatrix} \alpha_i \\ \alpha_j \\ \alpha_k \\ \cdot \\ \cdot \\ \cdot \end{Bmatrix} \tag{2.14}$$

$$= L\boldsymbol{\alpha} \quad \text{(say)}. \tag{2.15}$$

The displacement formulation (2.15) is in a suitable form for the finite element method. In addition to the stress function parameters, the vector $\boldsymbol{\alpha}$ can contain rigid body motion parameters, as appropriate. Such parameters do not appear in the stress function as they do not induce any stress. The strains are found by differentiating the displacements.

$$\boldsymbol{\epsilon} = \begin{Bmatrix} \epsilon_{rr} \\ \epsilon_{\theta\theta} \\ \gamma_{r\theta} \end{Bmatrix} = H\boldsymbol{\alpha}. \tag{2.16}$$

Columns of H corresponding to rigid body motion parameters are zero. The stresses are found from the strains using the generalised Hooke's Law.

$$\boldsymbol{\sigma} = \begin{Bmatrix} \sigma_{rr} \\ \sigma_{\theta\theta} \\ \tau_{r\theta} \end{Bmatrix} = D\boldsymbol{\epsilon} = DH\boldsymbol{\alpha}. \tag{2.17}$$

Consider a general finite element with N nodes surrounding a stress concentrator (see Fig. 1).

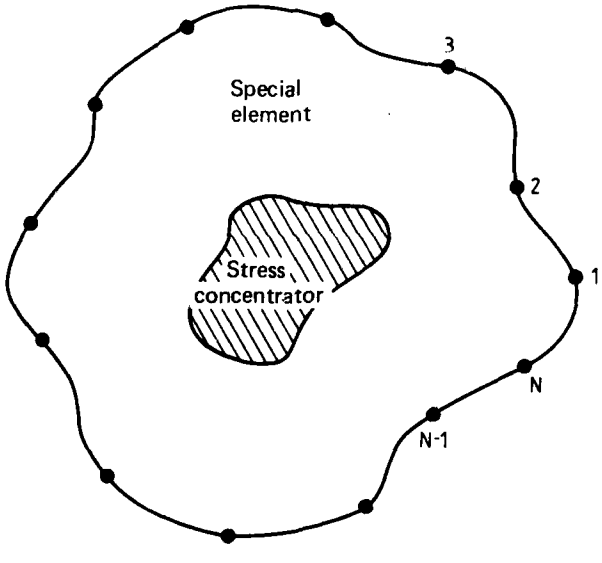

FIG 1: GENERALISED SPECIAL ELEMENT

The displacement formulation (2.15) applies to all points within the element, including the nodal points. Suppose (2.15) is applied to each of the N nodes in turn by substituting the appropriate co-ordinates into the matrix L. A vector of nodal point displacements can then be formed as:

$$\boldsymbol{\delta} = \begin{Bmatrix} d_1 \\ d_2 \\ \cdot \\ \cdot \\ \cdot \\ d_N \end{Bmatrix} = \begin{bmatrix} L_1 \\ L_2 \\ \cdot \\ \cdot \\ \cdot \\ L_N \end{bmatrix} \boldsymbol{\alpha} = C\boldsymbol{\alpha} \quad \text{(say)}. \tag{2.18}$$

If the number of arbitrary parameters chosen to form $\boldsymbol{\alpha}$ is equal to the number of nodal point displacement degrees of freedom, then the C matrix will be square. This enables the relationship (2.18) to be inverted.

$$\boldsymbol{\alpha} = C^{-1}\boldsymbol{\delta}. \tag{2.19}$$

In order to assemble this special element with the other elements forming the structure, it is necessary to derive a stiffness relationship between the nodal forces $\mathbf{q}$ and the nodal displacements $\boldsymbol{\delta}$.

$$\mathbf{q} = k\boldsymbol{\delta}. \tag{2.20}$$

The stiffness matrix k can be found by minimising the potential energy of the element, using the principle of virtual work.

$$k = (C^{-1})^T \int_V H^T D H dV C^{-1} \tag{2.21}$$

where the integration is over the volume of the element.

The relationship (2.20) can be readily transformed from local polar co-ordinates to global cartesian co-ordinates by using a transformation matrix, T.

$$\mathbf{q} = T\mathbf{Q}; \quad \boldsymbol{\delta} = T\boldsymbol{\Delta}. \tag{2.22}$$

$$\mathbf{Q} = T^T k T \boldsymbol{\Delta} \tag{2.23}$$

$$= K\boldsymbol{\Delta} \quad \text{(say)}. \tag{2.24}$$

Once the stiffness matrix K has been generated for a special element, it can be assembled with the other elements comprising the structure and a solution found for the displacements $\boldsymbol{\Delta}$ using a finite element program. The stresses can be calculated at any point within the element as:

$$\boldsymbol{\sigma} = DH\boldsymbol{\alpha} = DHC^{-1}T\boldsymbol{\Delta} = S\boldsymbol{\Delta} \quad \text{(say)}. \tag{2.25}$$

3. LOADED HOLE ELEMENT

3.1 General

A special element, to surround a circular hole with applied loading on its boundary, is described here (see also Ref. 1). The element is able to account accurately for applied loading by directly matching applied load and boundary stress distributions. The applied load distribution is represented as a finite Fourier series. Stress function coefficients of the element are related to the Fourier coefficients of the applied loading. The stress function formed from this relationship contains arbitrary parameters which lead to the formation of the element stiffness matrix, and fixed constants which lead to the formation of initial stresses and equivalent nodal forces to the applied loading. As would be expected, the stiffness matrix so formed is identical to that of an equivalent unloaded hole element. The influence of the applied loading is therefore expressed through the equivalent nodal forces and the initial stresses. The equivalent nodal forces are input loads for the finite element analysis, and the initial stresses are added to those calculated by the finite element analysis.

3.2 Element Shape

The basic shape of the element is an annulus with a polygonal outer boundary whose corners (nodes) lie on a circle concentric with the hole. The number of nodes and their angular co-ordinates can be varied, as can the aspect ratio of the circumscribing circle radius to the hole

radius. Three variants of this general shape are considered, according to the symmetry of the problem. For double symmetry only one quadrant is required, for single symmetry a semi-annulus, and for the unsymmetric case the full annulus. The three element variants are sketched in Figure 2. Also in Figure 2, the boundary conditions corresponding to the states of symmetry are shown. These boundary conditions actually alter the number of degrees of freedom of the element and that effect is also shown. The rigid body motions applicable to the three element variants are shown in Figure 2.

3.3 Fourier Analysis

The applied loading takes the form of normal and shear stresses, $\sigma_a(\theta)$ and $\tau_a(\theta)$, applied to the hole surface, $r = r_0$. The applied loads are represented by finite Fourier series as:

$$\sigma_a(\theta) = \sigma_{a0}/2 + \sum_{n=1}^{N_s} \{\sigma_{an} \cos n\theta + \sigma_{an} \sin n\theta\}. \tag{3.1}$$

$$\tau_a(\theta) = (\tau_{a0}/2) + \sum_{n=1}^{N_s} \{\tau_{an} \sin n\theta - \tau_{an} \cos n\theta\}. \tag{3.2}$$

The form of (3.2) is slightly different from the usual form of a finite Fourier series, (3.1), to simplify the imposition of boundary conditions in Section 3.4 below. The series cutoff, N_s, is selected large enough to obtain an adequate representation of $\sigma_a(\theta)$ and $\tau_a(\theta)$.

3.4 Boundary Conditions

The radial and shear stresses, derived[5] from the general stress function ϕ_n of Equation (2.5), are listed below.

$$\sigma_{rr} = [-a_n(n^2 - n)r^{n-2} - b_n(n^2 + n)r^{-n-2} - c_n(n^2 - n - 2)r^n - d_n(n^2 + n - 2)r^{-n}] \begin{Bmatrix} \sin n\theta \\ \cos n\theta \end{Bmatrix}. \tag{3.3}$$

$$\tau_{r\theta} = [a_n(n^2 - n)r^{n-2} - b_n(n^2 + n)r^{-n-2} + c_n(n^2 + n)r^n - d_n(n^2 - n)r^{-n}] \begin{Bmatrix} \cos n\theta \\ -\sin n\theta \end{Bmatrix}. \tag{3.4}$$

The single-valuedness requirement for a multiply-connected region restricts n to integer values. The boundary conditions for the loaded hole are:

$$\sigma_{rr} = \sigma_a(\theta) \text{ and } \tau_{r\theta} = \tau_a(\theta) \text{ at } r = r_0, \text{ all } \theta. \tag{3.5}$$

These boundary conditions are enforced by equating Fourier coefficients of the applied loading to stress function coefficients.

$$a_n(n^2 - n)r_0^{n-2} - b_n(n^2 + n)r_0^{-n-2} - c_n(n^2 - n - 2)r_0^n - d_n(n^2 + n - 2)r_0^{-n} = \sigma_{an}. \tag{3.6}$$

$$a_n(n^2 - n)r_0^{n-2} - b_n(n^2 + n)r_0^{-n-2} + c_n(n^2 + n)r_0^n - d_n(n^2 - n)r_0^{-n} = \tau_{an}. \tag{3.7}$$

Solving for a_n and c_n,

$$a_n = \frac{(n-2)\tau_{an} + n\sigma_{an}}{2(n^2 - n)r_0^{n-2}} - (n+1)r_0^{-2n}b_n - nr_0^{-2n-2}d_n. \tag{3.8}$$

$$c_n = \frac{\sigma_{an} - \tau_{an}}{2(n+1)r_0^n} + nr_0^{-2n-2}b_n + (n-1)r_0^{-2n}d_n. \tag{3.9}$$

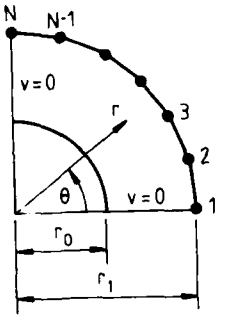

(a) Doubly symmetric (DS)

2N-2 degrees of freedom

v = 0 at $\theta = 0, \frac{\pi}{2}$ all r

No rigid body motion allowed

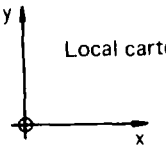

Local cartesian axes

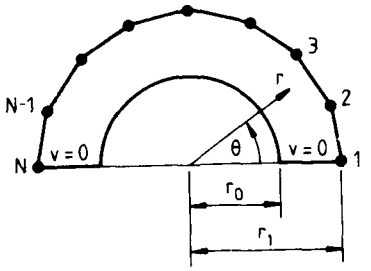

(b) Singly symmetric (SS)

2N-2 degrees of freedom

v = 0 at $\theta = 0, \pi$ all r

x translation rigid body motion only

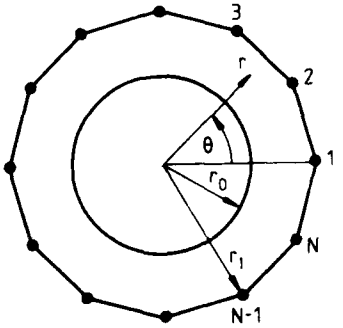

(c) Unsymmetric (US)

2N degrees of freedom

v unrestricted

All rigid body motions –

x and y translations and rotation

FIG 2: LOADED HOLE ELEMENT VARIANTS

Note that parameters a_n and c_n contain constant terms related to the applied loading but their relationships to parameters b_n and d_n are independent of the applied loading. Let the constant terms of parameters a_n and c_n be labelled s_{1n} and s_{2n} respectively:

$$s_{1n} = \frac{(n-2)\tau_{an} + n\sigma_{an}}{2(n^2-n)r_0^{n-2}}. \tag{3.10}$$

$$s_{2n} = -\frac{\sigma_{an} - \tau_{an}}{2(n-1)r_0^n}. \tag{3.11}$$

In Equations (3.6) to (3.11), the boundary conditions (3.5) have been imposed for the lower trigonometric functions of Equations (3.3) and (3.4). Let the parameters associated with the upper trigonometric functions of (3.3) and (3.4) be distinguished by a dash superscript, viz., a_n', b_n', c_n', d_n'. The boundary conditions (3.5) can be imposed in a similar manner for these parameters, and identical equations to (3.6) to (3.11) result, except that all parameters have dash superscripts, i.e. a_n', b_n', c_n', d_n', σ_{an}', τ_{an}', s_{1n}', s_{2n}'. The relationships (3.8) and (3.9) can be substituted into Equation (2.5) for the general stress function, ϕ_n.

$$\phi_n = \{[s_{1n}r^n + s_{2n}r^{2-n}] + [(n-1)r_0^{-2n}r^n + r^{-n} - nr_0^{2-2n}r^{2-n}]b_n + [nr_0^{2-2n}r^n + (n-1)r_0^{-2n}r^{2-n} - r^{2-n}]d_n\}\begin{Bmatrix}\sin n\theta\\ \cos n\theta\end{Bmatrix}, \tag{3.12}$$

i.e.

$$\phi_n = \phi_{n0} + \phi_{nH}. \tag{3.13}$$

Where ϕ_{n0} is a fixed stress function related to the applied loading, and ϕ_{nH} contains the arbitrary parameters b_n and d_n, and is the same stress function as for an unloaded hole. Stresses, strains and displacements can be derived from ϕ_n.

Special cases for $n = 0$ and 1 can be derived in the same manner as above, using the stress functions of (2.6), (2.7) and (2.8). Single-valuedness requires:

$$c_0 = d_0 = 0; \quad c_1 = -\frac{2}{1-\nu}d_1. \tag{3.14}$$

Then

$$\phi_0 = [a_0 + b_0\ln r + c_0r^2 + f_0\theta], \tag{3.15}$$

$$\sigma_{rr} = [b_0r^{-2} + 2c_0], \tag{3.16}$$

$$\tau_{r\theta} = [f_0r^{-2}], \tag{3.17}$$

so

$$b_0r_0^{-2} + 2c_0 = \sigma_{a0}/2, \tag{3.18}$$

and

$$f_0r_0^{-2} = \tau_{a0}/2. \tag{3.19}$$

Solving,

$$c_0 = \sigma_{a0}/4 - 0{\cdot}5r_0^{-2}b_0, \tag{3.20}$$

$$f_0 = 0{\cdot}5r_0^2\tau_{a0}, \tag{3.21}$$

$$s_{10} = 0{\cdot}5r_0^2\tau_{a0}; \quad s_{20} = \sigma_{a0}/4, \tag{3.22}$$

$$\phi_{00} = [s_{10}\theta + s_{20}r^2], \tag{3.23}$$

$$\phi_{0H} = [\ln r - 0{\cdot}5(r/r_0)^2]b_0, \tag{3.24}$$

$$\phi_1 = [a_1r + b_1r^{-1} + c_1r^3 + d_1r\ln r]\begin{Bmatrix}\sin\theta\\ \cos\theta\end{Bmatrix} - d_1\frac{2r\theta}{1-\nu}\begin{Bmatrix}\cos\theta\\ \sin\theta\end{Bmatrix}, \tag{3.25}$$

$$\sigma_{rr} = [\quad 2b_1 r^{-3} + 2c_1 r^{-1} - \frac{3+\nu}{1+\nu} d_1 r^{-1}] \begin{Bmatrix} \sin\theta \\ \cos\theta \end{Bmatrix}, \tag{3.26}$$

$$\tau_{r\theta} = [\quad 2b_1 r^{-3} + 2c_1 r^{-1} + d_1 r^{-1}] \begin{Bmatrix} \cos\theta \\ \sin\theta \end{Bmatrix}, \tag{3.27}$$

$$c_1 = \frac{(1-\nu)\sigma_{a1} + (3+\nu)\tau_{a1}}{8r_0} - r_0^{-1} b_1, \tag{3.28}$$

$$d_1 = \frac{(1+\nu)(\tau_{a1} - \sigma_{a1})r_0}{4}, \tag{3.29}$$

$$s_{11} = \frac{(1-\nu)\sigma_{a1} + (3+\nu)\tau_{a1}}{8r_0} - \quad ; \quad s_{21} = d_1, \tag{3.30}$$

$$\phi_{1n} = [s_{11} r^{1} + s_{21} r \ln r] \begin{Bmatrix} \sin\theta \\ \cos\theta \end{Bmatrix} \quad s_{21} \frac{2r\theta}{1+\nu} \begin{Bmatrix} \cos\theta \\ \sin\theta \end{Bmatrix}, \tag{3.31}$$

$$= [r^{-1} - r_0^{-3} r^{1}] b_1 \begin{Bmatrix} \sin\theta \\ \cos\theta \end{Bmatrix}. \tag{3.32}$$

3.5 Arbitrary Parameters

It remains to choose values of n to form the vector $\boldsymbol{\alpha}$ of the arbitrary parameters b_n and d_n. The rule followed is to choose consecutive allowable values of n, ranging from the lowest, until all the available degrees of freedom of the element have been filled. The allowable values of n and the applicability of the upper and lower trigonometric functions (dashed and undashed parameters) are determined by conditions of symmetry. Symmetry conditions can be expressed as additional boundary conditions. These are listed below for the three loaded hole element variants (see Fig. 2).

$$\text{unsymmetric: no restriction,} \tag{3.33}$$

$$\text{singly symmetric: } t = 0 \text{ at } \theta = 0, \pi, \text{ all } r, \tag{3.34}$$

$$\text{doubly symmetric: } t = 0 \text{ at } \theta = 0, \tfrac{1}{2}\pi, \text{ all } r. \tag{3.35}$$

These boundary conditions affect the number of degrees of freedom of the element. Normally, if an element has N nodes it has $2N$ degrees of freedom, corresponding to u and v displacements at each node. However, (3.34) and (3.35) suppress the v displacement at the first and last nodes, leaving the singly and doubly symmetric variants with only $2N-2$ degrees of freedom. Consequently, when the C matrix is evaluated according to (2.18), the v displacement is not included in $\mathbf{d}_1$ and $\mathbf{d}_N$. Finally, the applicable rigid body motion components have to be included. All these factors have to be accounted for in forming $\boldsymbol{\alpha}$ and the result is shown in Table 1 for elements with N nodes. The notation for the rigid body motion components is shown in Table 2.

3.6 Fixed Parameters

It is convenient to assemble the fixed parameters, s_{1n} and s_{2n}, related to the applied loading, into a vector $\boldsymbol{\alpha}_0$ (say), in the same manner as the arbitrary parameters are assembled into $\boldsymbol{\alpha}$. For the general case, from (3.12) and (3.13) we have:

$$\phi_{n0} = [s_{1n} r^{n} + s_{2n} r^{2-n}] \begin{Bmatrix} \sin n\theta \\ \cos n\theta \end{Bmatrix} \tag{3.36}$$

$$= s_{1n} r^{n} \begin{Bmatrix} \sin n\theta \\ \cos n\theta \end{Bmatrix} + s_{2n} r^{2-n} \begin{Bmatrix} \sin n\theta \\ \cos n\theta \end{Bmatrix} \tag{3.37}$$

$$= s_{1n} f_{1n}(r,\theta,n) + s_{1n} f_{1n} + s_{2n} f_{2n} + s_{2n} f_{2n} \tag{3.38}$$

$$= [f_{1n}, f_{2n}, f_{1n}, f_{2n}] \begin{Bmatrix} s_{1n} \\ s_{2n} \\ s_{1n} \\ s_{2n} \end{Bmatrix} \tag{3.39}$$

$$= F_{n0} \boldsymbol{\alpha}_{n0} \quad \text{(say)}. \tag{3.40}$$

TABLE 1

Loaded Hole Element Parameters

	Doubly symmetric	Singly symmetric	Unsymmetric
Additional boundary conditions	$v = 0$ at $\theta = 0, \frac{1}{2}\pi$ all r	$v = 0$ at $\theta = 0, \pi$ all r	None
Appropriate functions for ϕ; $n = 0, 1, 2, \ldots$	$\cos 2n\theta$	$\cos n\theta$	$\sin (n-1)\theta$ $\cos n\theta$
Applicable rigid body motions	None	β_1 only	All
Element degrees of freedom	$2N-2$	$2N-2$	$2N$
$\{x\}$	$\begin{Bmatrix} b_0 \\ b_2 \\ d_2 \\ b_4 \\ d_4 \\ \cdot \\ \cdot \\ \cdot \\ \cdot \\ b_{2N-4} \\ d_{2N-4} \\ b_{2N-2} \end{Bmatrix}$	$\begin{Bmatrix} b_0 \\ b_1 \\ b_2 \\ d_2 \\ b_3 \\ d_3 \\ \cdot \\ \cdot \\ \cdot \\ \cdot \\ \cdot \\ b_{N-2} \\ d_{N-2} \\ b_{N-1} \\ \beta_1 \end{Bmatrix}$	N odd $\begin{Bmatrix} \cdot \\ \cdot \\ \cdot \\ b_{(N-1)/2} \\ d_{(N-1)/2} \\ b_{(N-1)/2} \\ d_{(N-1)/2} \\ \beta_1 \\ \beta_2 \\ \beta_3 \end{Bmatrix}$ $\begin{Bmatrix} b_0 \\ b_1 \\ b_1' \\ b_2 \\ d_2 \\ b_2 \\ d_2 \\ \cdot \\ \cdot \\ \cdot \end{Bmatrix}$ N even $\begin{Bmatrix} \cdot \\ \cdot \\ \cdot \\ \cdot \\ b_{N/2-1} \\ d_{N/2-1} \\ b_{N/2-1} \\ d_{N/2-1} \\ b_{N/2} \\ b_{N/2} \\ \beta_1 \\ \beta_2 \\ \beta_3 \end{Bmatrix}$

TABLE 2

Rigid Body Motion Parameters

Rigid body motion	Notation	u	v
x translation	β_1	$\beta_1 \cos\theta$	$\beta_1 \sin\theta$
y translation	β_2	$\beta_2 \sin\theta$	$\beta_2 \cos\theta$
Rotation	β_3	0	$\beta_3 r$

Now, if the total stress function matching the applied loading is written as:

$$\phi_0 = \Sigma \phi_{n0}, \tag{3.41}$$

then

$$\phi_0 = \Sigma F_{n0}\alpha_{n0} = F_0\alpha_0. \tag{3.42}$$

Displacements, strains and stresses can be derived from (3.42) as:

$$\mathbf{d}_0 = L_0\boldsymbol{\alpha}_0, \tag{3.43}$$

$$\boldsymbol{\epsilon}_0 = H_0\boldsymbol{\alpha}_0, \tag{3.44}$$

$$\boldsymbol{\sigma}_0 = DH_0\boldsymbol{\alpha}_0. \tag{3.45}$$

The appropriate functions for ϕ as given in Table 1, are applicable to ϕ_0 also, since the symmetry of the applied loading is an integral factor of the overall symmetry. However, it is not necessary for the number of parameters in $\boldsymbol{\alpha}_0$ to match those in $\boldsymbol{\alpha}$. The parameter series in $\boldsymbol{\alpha}_0$ is cut off at a point where an adequate representation of the applied loading is obtained. For special applied load distributions, $\boldsymbol{\alpha}_0$ may contain only one or a few non-zero parameters. Rigid body motion parameters are not applicable for $\boldsymbol{\alpha}_0$.

3.7 Stiffness Equation

It has been shown that the total stress function for the element can be expressed as:

$$\phi = \phi_0 + \phi_H. \tag{3.46}$$

From this, it follows that

$$\mathbf{d} = \mathbf{d}_0 + \mathbf{d}_H, \tag{3.47}$$

$$= L_0\boldsymbol{\alpha}_0 + L_H\boldsymbol{\alpha}_H, \tag{3.48}$$

and

$$\boldsymbol{\delta} = C_0\boldsymbol{\alpha}_0 + C_H\boldsymbol{\alpha}_H, \tag{3.49}$$

so

$$\boldsymbol{\alpha}_H = -C_H^{-1}C_0\boldsymbol{\alpha}_0 + C_H^{-1}\boldsymbol{\delta}. \tag{3.50}$$

Also,

$$\boldsymbol{\epsilon} = H_0\boldsymbol{\alpha}_0 + H_H\boldsymbol{\alpha}_H, \tag{3.51}$$

so

$$\boldsymbol{\sigma} = D\boldsymbol{\epsilon} = DH_0\boldsymbol{\alpha}_0 + DH_H\boldsymbol{\alpha}_H, \tag{3.52}$$

$$= DH_0\boldsymbol{\alpha}_0 + DH_H(-C_H^{-1}C_0\boldsymbol{\alpha}_0 + C_H^{-1}\boldsymbol{\delta}), \tag{3.53}$$

$$= D(H_0 - H_HC_H^{-1}C_0)\boldsymbol{\alpha}_0 + DH_HC_H^{-1}\boldsymbol{\delta}. \tag{3.54}$$

Now impose a virtual displacement, $\boldsymbol{\delta}^*$.

$$\mathbf{d}^* = L_HC_H^{-1}\boldsymbol{\delta}^*, \tag{3.55}$$

$$\boldsymbol{\epsilon}^* = H_HC_H^{-1}\boldsymbol{\delta}^*. \tag{3.56}$$

Consider the energy changes due to $\boldsymbol{\delta}^*$. Let $\mathbf{q}$ be the vector of element nodal forces and $\mathbf{p}$ the vector of applied body forces.

(1) External work done on the element:

$$\text{by } \mathbf{q}, \qquad W_E^1 = (\boldsymbol{\delta}^*)^T\mathbf{q}, \tag{3.57}$$

$$\text{by } \mathbf{p}, \qquad W_E^2 = \int_\Lambda (\mathbf{d}^*)^T\mathbf{p}\,d\Lambda, \tag{3.58}$$

(2) Internal work:

$$W_I = \int_\Lambda (\boldsymbol{\epsilon}^*)^T\boldsymbol{\sigma}\,d\Lambda. \tag{3.59}$$

For equilibrium,

$$W_E^1 + W_E^2 = W_I. \tag{3.60}$$

i.e.

$$(\delta^*)^T\mathbf{q} + \int_v (\mathbf{d}^*)^T\mathbf{p}dv = \int_v (\epsilon^*)^T\sigma dv, \tag{3.61}$$

$$(\delta^*)^T\mathbf{q} = \int_v (H_H C_H^{-1}\delta^*)^T(DH_0\alpha_0 - DH_H C_H^{-1}C_0\alpha_0 + DH_H C_H^{-1}\delta)dv -$$

$$-\int_v (L_H C_H^{-1}\delta^*)^T\mathbf{p}dv. \tag{3.62}$$

$$(\delta^*)^T\mathbf{q} = (\delta^*)^T(C_H^{-1})^T\int_v (H_H^T DH_0\alpha_0 - H_H^T DH_H C_H^{-1}C_0\alpha_0 + H_H^T DH_H C_H^{-1}\delta)dv -$$

$$-(\delta^*)^T(C_H^{-1})^T\int_v L_H^T\mathbf{p}dv. \tag{3.63}$$

Since δ^* is arbitrary,

$$\mathbf{q} = (C_H^{-1})^T\int_v H_H^T DH_0 dv\alpha_0 - (C_H^{-1})^T\int_v H_H^T DH_H dv C_H^{-1}C_0\alpha_0 +$$

$$+(C_H^{-1})^T\int_v H_H^T DH_H dv C_H^{-1}\delta - (C_H^{-1})^T\int_v L_H^T\mathbf{p}dv. \tag{3.64}$$

The first two terms on the right-hand side of (3.64) are vectors of nodal forces related to the initial stresses of Equation (3.54). When these terms were numerically evaluated in Reference 1 they proved to be self cancelling. That result was not able to be proved analytically in Reference 1. However, those two terms are neglected in this paper as having no effect. The third term on the right-hand side of (3.64) contains the stiffness matrix of the element (see (2.21)). The last term is the standard formulation of the vector of nodal forces $\mathbf{q}_0$, equivalent to the applied loading (see Ref. 2). Hence, (3.64) reduces to:

$$\mathbf{q} = k\delta - \mathbf{q}_0. \tag{3.65}$$

Equation (3.65) can be converted to global cartesian co-ordinates using a transformation, T (see (2.22) to (2.24)).

$$\mathbf{Q} = K\Delta - \mathbf{Q}_0. \tag{3.66}$$

Stress recovery is achieved through Equation (3.54) which may be written as:

$$\sigma = \sigma_0 + s\delta, \tag{3.67}$$

$$= \sigma_0 + S\Delta. \tag{3.68}$$

Equation (3.68) can be evaluated at a number of prescribed points and assembled as shown below.

$$\begin{Bmatrix}\sigma_1\\ \sigma_2\\ \cdot\\ \cdot\\ \cdot\end{Bmatrix} = \begin{Bmatrix}(\sigma_0)_1\\ (\sigma_0)_2\\ \cdot\\ \cdot\\ \cdot\end{Bmatrix} + \begin{bmatrix}S_1\\ S_2\\ \cdot\\ \cdot\\ \cdot\end{bmatrix}\Delta \tag{3.69}$$

i.e.

$$\sigma_T = \sigma_{0T} + S_T\Delta \quad \text{(say)}. \tag{3.70}$$

3.8 Stiffness Matrix Evaluation

The main step in evaluating the stiffness matrix of an element is to evaluate the volume integral of Equation (2.21). That integral is given the notation:

$$G = \int_v H^T DH dv. \tag{3.71}$$

For the loaded hole element, the volume of integration is an annulus of uniform thickness, with a circular inner boundary and a possibly irregular, polygonal outer boundary. In view of the complexity of the terms in the H matrix (see Ref. 1), it is not feasible to evaluate this integral analytically. The method of integration chosen is to approximate the outer polygonal boundary by a circular one, concentric with the hole, without changing the volume of the element. This allows the integration to be performed between constant limits for r and θ. The equivalent outer radius is given by:

$$r_{EQ} = r_1\left\{\frac{1}{2\pi f}\sum_{i=1}^{N-1}\sin(\gamma_{i+1} - \gamma_i)\right\}^{1/2}, \tag{3.72}$$

where $f = 0{\cdot}25$ and $0{\cdot}5$ for the doubly and singly symmetric cases respectively, and:

$$r_{EQ} = r_1\left\{\frac{1}{2\pi f}\left(\sum_{i=1}^{N-1}\sin(\gamma_{i+1} - \gamma_i) + \sin(\gamma_1 - \gamma_N)\right)\right\}^{1/2}, \tag{3.73}$$

where $f = 1{\cdot}0$ for the unsymmetric case; γ_i is the angular co-ordinate of node i. Now (3.71) becomes:

$$G = b\int_{r_0}^{r_{EQ}} r\,dr\int_0^{2f\pi} H^T D H\,d\theta, \tag{3.74}$$

where b is the thickness of the element. It was shown in Reference 1 that the integral over θ is readily performed analytically, resulting in a diagonal type matrix. The integration over r is more complex and is performed numerically.

4. COMPUTER PROGRAM DESCRIPTION

A computer program has been written to generate the matrices and vectors K, S_T, $\mathbf{Q}_0$ and $\boldsymbol{\sigma}_{0T}$ of Equations (3.66) and (3.70), for a specified loaded hole element. The program was written in Fortran for use on the PDP-10 computer of the Aeronautical Research Laboratories, in conjunction with the general purpose finite element analysis program, DISMAL.[6] The program, entitled "HOLE", has been entered in the ARL Computer Program Register and a listing and other details of the program are contained therein.

The program requires one input file and generates three output files. The input file, HIN, contains a geometric description of the element, material properties, prescribed points for stress evaluation, and applied loading definition. For precise details of the input file structure and a listing of a typical input file, see Appendix B. Two of the output files are for direct use by DISMAL. DATA.EXT is an ASCII file containing bookkeeping information, and SPIT is a binary file containing the stiffness and stress matrices, K and S_T. These files are written in APPEND mode so that, by re-running the program, the properties of several loaded hole elements can be strung together for access by DISMAL. The third output file, LOADS, contains the equivalent nodal forces $\mathbf{Q}_0$, the initial stresses $\boldsymbol{\sigma}_{0T}$, C matrix inversion parameters, and the global stiffness matrix K, all in ASCII form and self explanatory format. Operating instructions for the loaded hole element program in conjunction with DISMAL are given in Appendix C.

The program caters for three modes of specifying the applied loading (see Appendix A.) Firstly, Fourier coefficients can be input directly. The program user must c sure that the input coefficients conform to the allowable functions appropriate to the particular loaded hole element variant (see Table 1). Secondly, point loads at various angular co-ordinates can be specified. The program automatically allows for symmetry in calculating the Fourier coefficients for point loads, by excluding inappropriate coefficients. Finally, for general distributed loading, the program reads ordinate values at an odd number of equally distributed points around the hole boundary. Again, the program automatically enforces symmetry. For the double and singly symmetric variants a reflected set of ordinates is generated from the input ordinates. The program obtains the Discrete Fourier Transform of the ordinate values by calling a subroutine entitled C06AAF from the NAG library of subroutines available on the PDP-10 computer at ARL. For the doubly symmetric variant the frequencies of the computed Fourier coefficients are doubled, to allow for the fact that the input and reflected ordinate values cover a range π rather than 2π. For representing the applied loads, it has proved necessary to use $n = 8$ as a limiting

frequency, as inclusion of higher frequency coefficients introduces large numerical errors into the calculation of the initial stress $\boldsymbol{\sigma}_0$. The program caters for the specification of no applied loading, in which case it functions as an unloaded hole element. No equivalent nodal forces or initial stresses are then output.

The integration over r of Equation (3.74) is performed numerically, using Simpson's rule with 100 points. The inversion of the matrix C_{H} of Equations (3.49) and (3.64) is performed by a subroutine, GENINV.[7]

The points at which the vector $\boldsymbol{\sigma}_0$ and the matrix S of (3.67) are evaluated, to construct the vector $\boldsymbol{\sigma}_{0\mathrm{T}}$ and the matrix S_{T} of (3.70), consist of radial projections of the nodal points onto the hole boundary, other prescribed points on the hole boundary, and general prescribed points. For points on the hole boundary, only the tangential stress component is included in $\boldsymbol{\sigma}_{0\mathrm{T}}$ and S_{T}, as the radial and shear stress components are known from the applied loading. Co-ordinates of prescribed points are defined in the input file to the program.

In principle, it is not necessary to have a uniform distribution of nodes around the circumscribing circle of the element. However, unexplained numerical difficulties have been encountered when using the program with non-uniform distributions of nodes (see Ref. 1). Therefore, the use of the current loaded hole element program is restricted to uniform distributions only. The aspect ratio of the element, r_1/r_0, is unrestricted except to be greater than unity. However, results of example analyses indicate that this ratio should be in the range 1·5 to 3·0 for best accuracy (see Ref. 1). Other restrictions on the input data, necessary for satisfactory operation of the program, are listed in Appendix B.

5. EXAMPLE ANALYSES

5.1 Problems and Results

Many example analyses were described in Reference 1. Some of those are included in this section in order to demonstrate the use of the element and the accuracy to be expected from it. The first example is a rectangular plate with a central circular hole, subject to uniform longitudinal tension (see Fig. 3). This is a doubly symmetric problem and the mesh used is shown in Figure 3. A doubly symmetric hole element with eight uniformly spaced nodes was used. The maximum stress concentration around the hole boundary is of interest, i.e. the tangential stress $\sigma_{\theta\theta}$ at $r = r_0$, $\theta = 0$ divided by the uniform applied stress. Accurate values for this stress concentration factor, accounting for the finite width of the plate but not the finite length, are available in Reference 8. This problem was analysed for a range of values of r_0, keeping the element circumscribing radius, r_1, constant. Zero applied loading was specified for the hole element. The results are shown in Table 3.

TABLE 3

Stress Concentration for Hole in a Rectangular Plate

r_0	r_1/r_0	$(\sigma_{\theta\theta})_{\max}/\sigma$	$(\mathrm{s.c.f.})_{\mathrm{acc}}$*	v_0 error
1·0	4·0	3·56	3·02	17·8
1·25	3·2	3·02	3·04	0·7
1·5	2·67	3·05	3·05	0·0
2·0	2·0	3·12	3·10	0·7
2·5	1·6	3·20	3·16	1·2
3·0	1·33	3·30	3·24	1·9
3·5	1·14	3·44	3·34	3·0

* Accurate value of stress concentration factor, $(\sigma_{\theta\theta})_{\max}/\sigma$, obtained from Reference 8.

The performance of the singly symmetric variant of the loaded hole element is demonstrated by the problem of an offset circular hole in a circular disc, subject to uniform internal pressure.

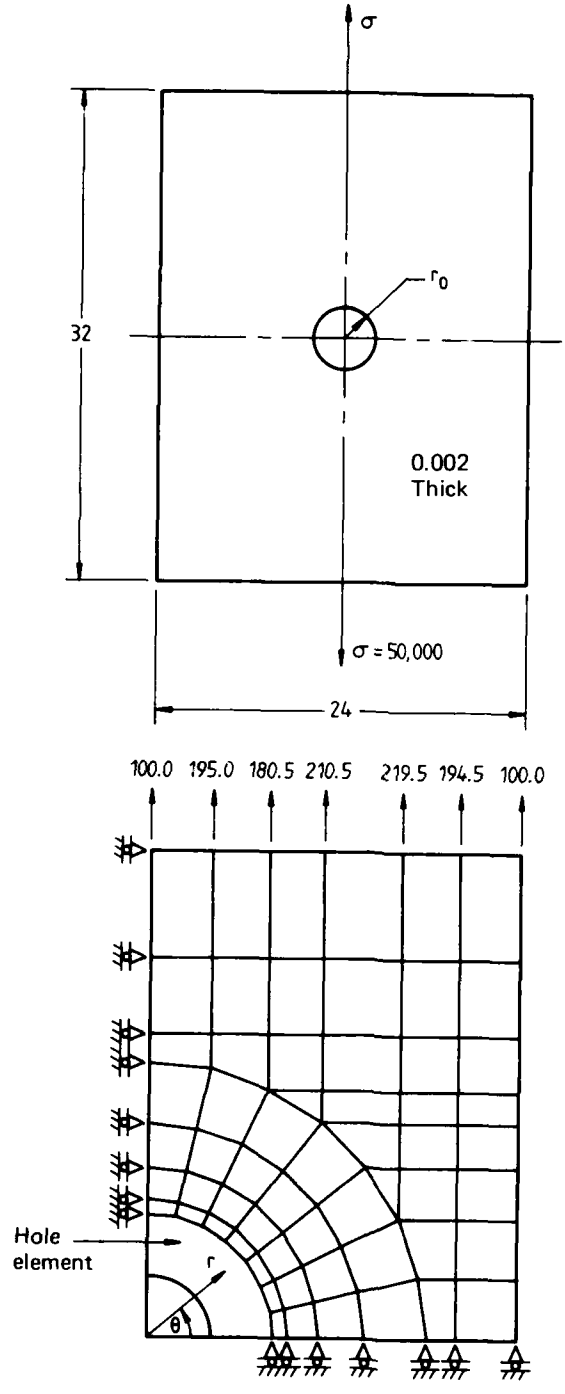

FIG 3: HOLE IN RECTANGULAR PLATE

The mesh used is shown in Figure 4. Uniform internal pressure of 1.0×10^5 is specified by inputting the frequency coefficient $\sigma_{an} = 2.0 \times 10^5$ with $n = 0$ (see Appendix B). Accurate values for the stress concentration factor at points A and B of Figure 4 have been obtained from Reference 8. Values derived from the analysis of the mesh of Figure 4 have been compared to them in Table 4.

TABLE 4

Stress Concentration for an Offset Hole

Point	σ_{mn}/p_0	$(\text{s.c.f.})_{\text{acc}}$	% error
A	2·11	2·17	2·8
B	1·68	1·65	1·8

An example problem with a broad spectrum of frequency components in the loading applied to the hole, is a riveted joint with load transfer through the rivets. The load distribution is of cosine form over the area of contact between the rivet and the hole. This problem is detailed in Figure 5. For the riveted joint problem the applied loading was input as ordinate values and the frequency components established by taking the DFT. The tangential stress was calculated at many points around the hole boundary and the maximum stress concentration factor, $K_{mb} = \frac{\sigma_{mn}}{\sigma}\left(\frac{a}{b}\right)$ was found to be 2·15 at $\theta = 58^\circ$. This is 5·7% in error with an accurate value of 2·28 at $\theta = 60^\circ$ given in Reference 8.

The versatility of the loaded hole element is demonstrated by the analysis of two holes, of generally unequal diameter, in a large plate (effectively infinite). The mesh used is shown in Figure 6. For each run of the problem two load cases were analysed, viz. each hole in turn subject to uniform internal pressure p_0 with the other hole unloaded. From run to run, the radii of the holes were varied without altering the mesh and keeping r_1/r_0 in the range 1·5 to 3·0. For either load case of any run, the maximum tangential stress occurs at a point C on the loaded hole surface, displaced by an angle θ_c from the line joining the hole centres. The stress concentrations at point A on the loaded hole boundary and point B on the unloaded hole boundary are also of interest. Points A, B and C are illustrated in Figure 7. The results from all runs are given in Table 5 where the subscript 1 refers to the loaded hole and the subscript 2 to the unloaded hole. The stress concentrations at point C in Table 5 have been plotted in Figure 7. For the combined loading case of both holes under equal pressure when $r_{01} = r_{02}$, the stress concentration at points A and B can be found by adding the values in columns A and B of Table 5. These combined values are compared with accurate values from Reference 8 in Table 6.

5.2 Discussion of Results

The example analyses outlined in the preceding section demonstrate the accuracy and utility of the loaded hole element. The first example, a central hole in a rectangular plate, indicates that, for best accuracy, the aspect ratio of the element, r_1/r_0, should be kept in the range 1·5 to 3·0. For that problem, errors were then less than 2%. The analysis of the riveted joint shows that the element can produced accurate stress concentration values, even for complex applied load distributions. The mesh for that problem, shown in Figure 5, uses several six-noded triangular elements, two of which adjoin the loaded hole element. The two mid-side nodes along the junction are not nodes of the hole element. Unconnected nodes are normally undesirable as introducing inter-element displacement incompatibility. However, with standard element connections to the loaded hole element, displacement incompatibility is inevitable anyway, and using unconnected nodes will not necessarily worsen it. The analysis of two adjacent holes in an infinite plate shows the flexibility of the loaded hole element. Using only one mesh, broad ranges of the basic parameters of the problem were spanned, with errors less than 3%. An alternate solution of this problem is unknown, and the stress concentration values in Table 5 are then useful basic data.

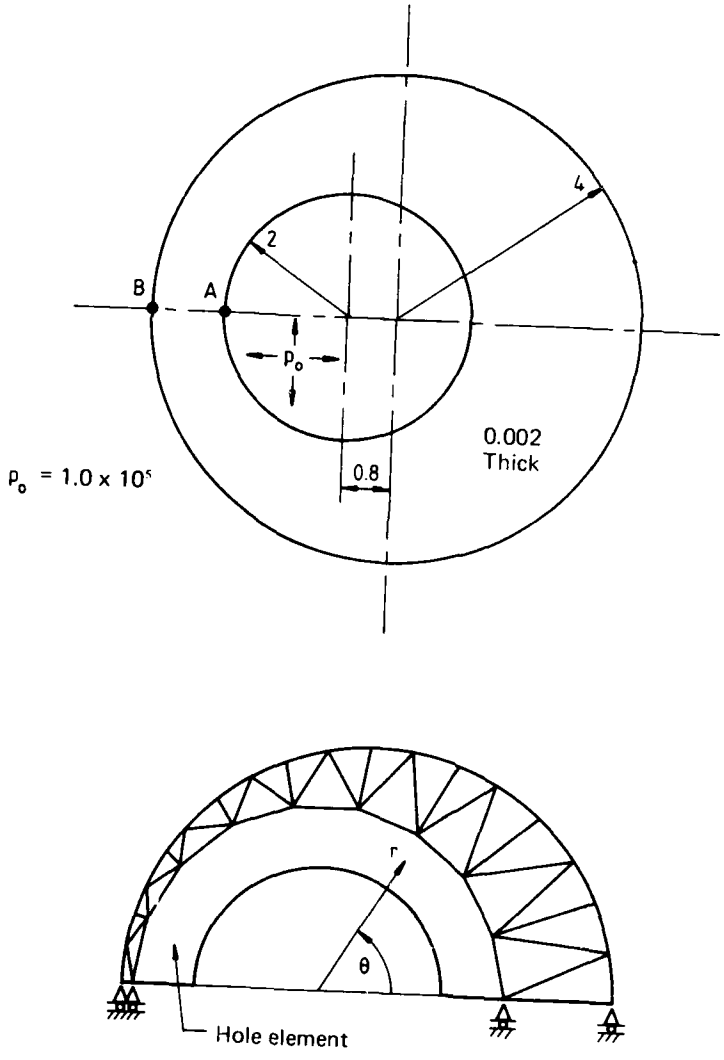

FIG 4: OFFSET HOLE IN CIRCULAR DISC

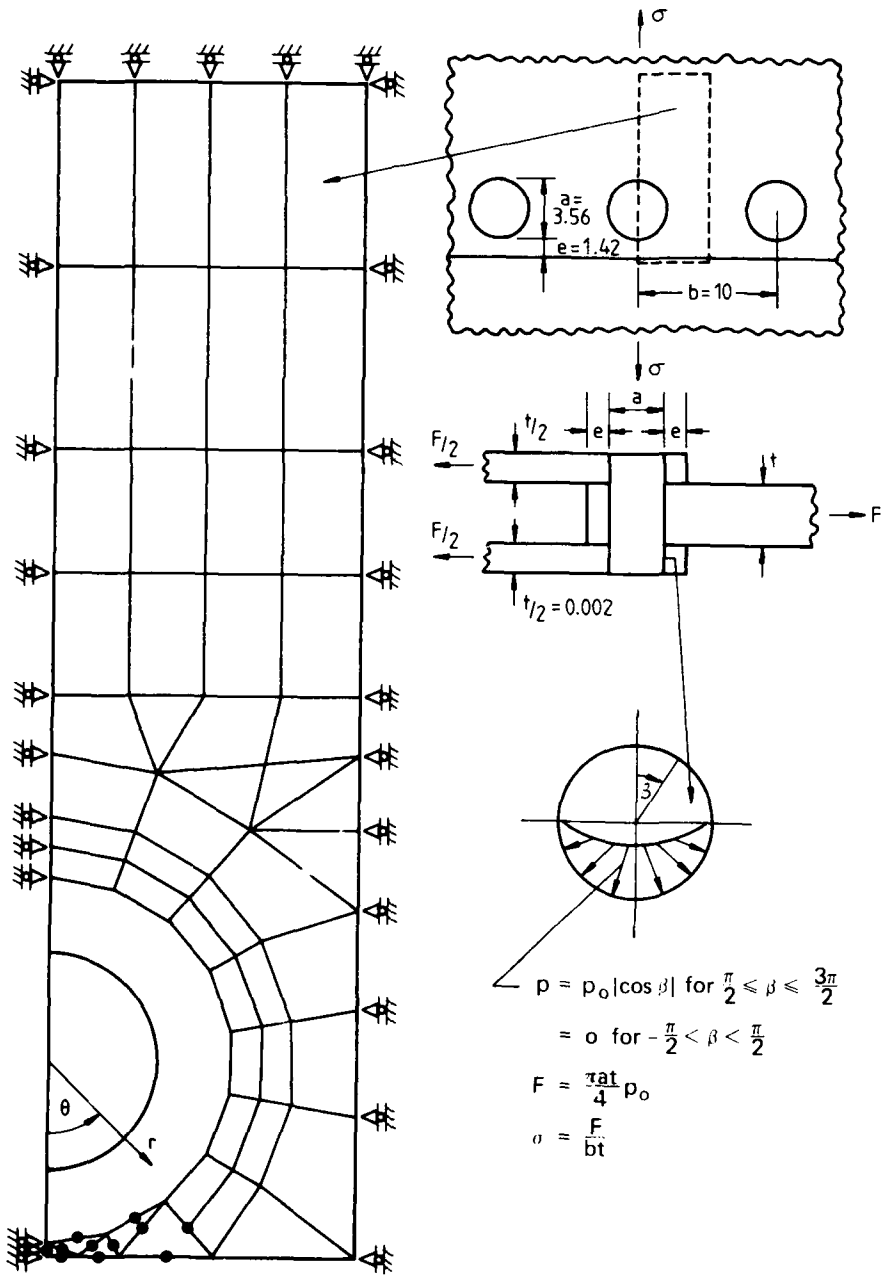

FIG 5: RIVETED JOINT

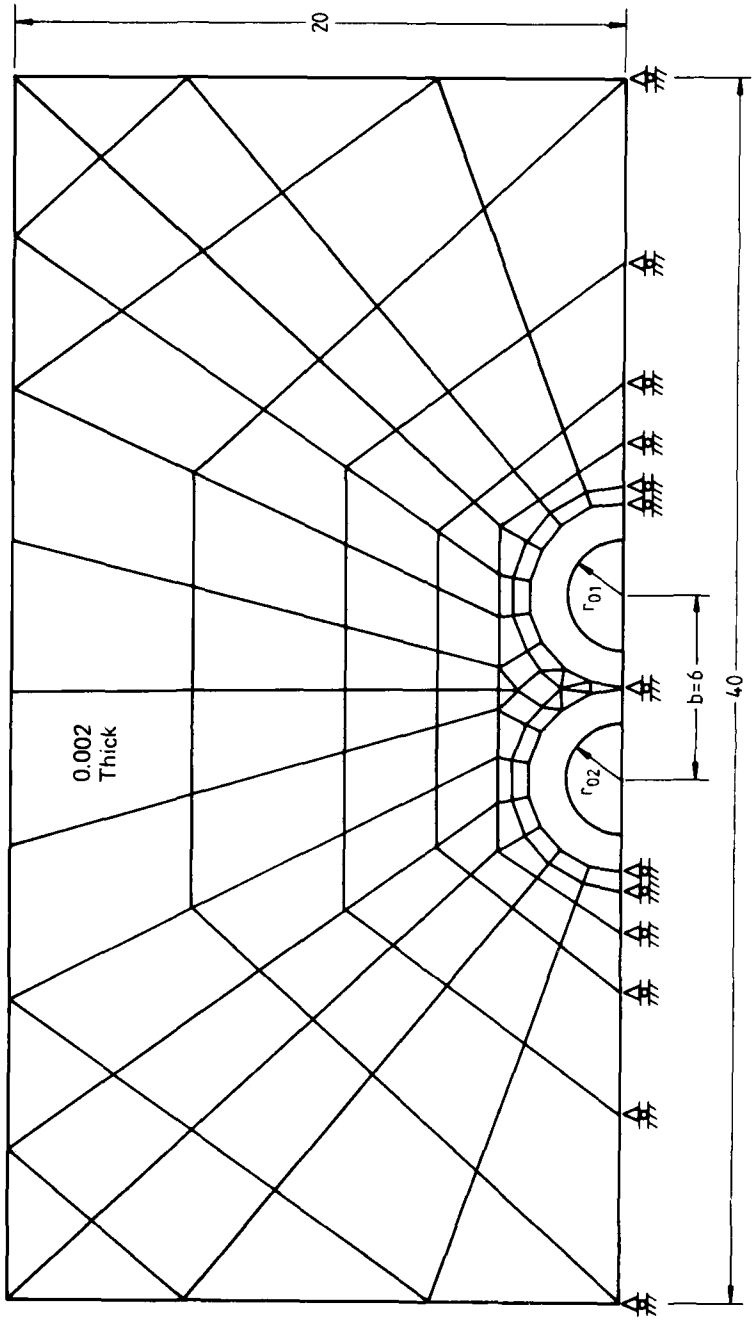

FIG 6: TWO HOLES IN AN INFINITE PLATE

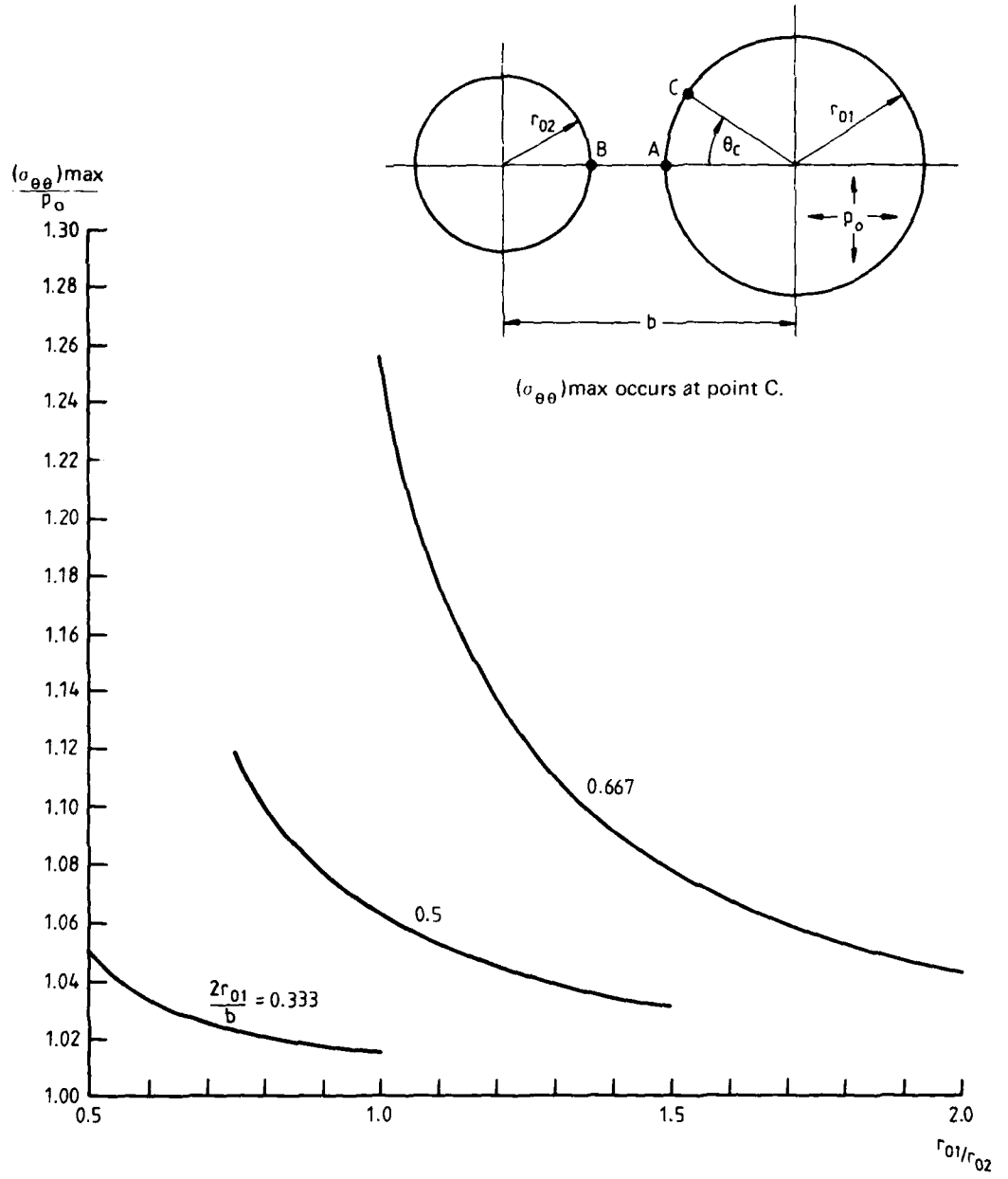

FIG 7: STRESS CONCENTRATION FOR TWO HOLES IN AN INFINITE PLATE

TABLE 5

Stress Concentration for Two Holes in an Infinite Plate

r_{01}	r_{02}	r_{01}/r_{02}	$2r_{01}\ b$	$\sigma_{\theta\theta}/p_0$			θ_C (deg)
				A	B	C	
1·0	1·0	1·0	0·333	1·007	0·163	1·014	70
1·0	1·5	0·667	0·333	1·000	0·199	1·027	60
1·5	1·0	1·5	0·5	0·979	0·374	1·031	80
1·0	2·0	0·5	0·333	0·989	0 249	1·050	60
2·0	1·0	2·0	0·667	0·963	0·664	1·042	80
1·5	1·5	1·0	0·5	0·991	0·460	1·062	60
1·5	2·0	0·75	0·5	0·953	0·589	1·118	60
2·0	1·5	1·333	0·667	0·906	0·835	1·103	40
2·0	2·0	1·0	0·667	0·866	1·093	1·254	40

TABLE 6

Stress Concentration for Two Equal Holes in an Infinite Plate

$r_{01} = r_{02}$	$b\ 2r_{01}$	$(\sigma_{\theta\theta}/p_0)_{\text{Point A}}$		% error
		Hole element	Reference 8	
1·0	3	1·170	1·153	1·5
1·5	2	1·451	1·410	2·9
2·0	1·5	1·959	1·900	3·1

The errors listed in Table 6 can be considered as upper limits on the possible errors in Table 5.

6. DISCUSSION

The loaded hole element has many advantages over an equivalent mesh of standard elements. Firstly, stresses can be obtained accurately at any point within the element. Specifically, the process of matching boundary stresses with applied loads ensures accurate stresses, at or near the boundary. Standard elements cannot produce boundary stresses, no matter how much the mesh is refined. In order to obtain boundary stresses from them, it is necessary to extrapolate to the boundary, and in the case of a hole boundary, the extrapolation is into a region of high stress gradients. When using the loaded hole element, both preparation and computing time are

cut significantly from an equivalent analysis with a standard element mesh. This is due to a reduction in the number of elements and nodes. The displacement incompatibility of the loaded hole element with adjoining standard elements did not prove to be a significant factor. Bounds on the accuracy of the solutions to example problems were not established, due to the oscillatory nature of the convergence. However, for most engineering applications, all that is required is a knowledge of the expected accuracy of the analysis, and experience in that regard can be gained from comparisons of analyses using the loaded hole element with theoretical solutions (see Section 5).

As mentioned in the introduction to this report, the hole element was developed as a stage in the development of an element capable of representing a warhead fragment damage site in an aircraft structure. Such a damage site can be idealised as a hole with cracks radiating from it. As yet, endeavours to extend the hybrid element method to model a hole with one or two long cracks radiating from it have met with numerical difficulties, and this goal has had to be left for later study.

7. CONCLUSION

The satisfactory operation of the three variants of the loaded hole element has been confirmed for uniform distributions of 4 to 10 nodes. Adequate operating instructions for the loaded hole element program are contained in Appendices B and C to this report. A listing of the program is contained in the ARL Computer Program Register.

REFERENCES

1. Watters, K. C.: "Developments in Hole Elements", M.Eng.Sc. Thesis, University of Melbourne, April 1980.
2. Zienkiewicz, O. C.: *The Finite Element Method in Engineering Science*. McGraw-Hill, 1971.
3. Rao, A. K., Raju, I. S., and Krishna Murty, A. V.: "A Powerful Hybrid Method in Finite Element Analysis", *Int. J. for Numerical Methods in Eng.*, **3**, 1971.
4. Rao, A. K., Raju, I. S., and Krishna Murty, A. V.: "Sector Elements for Matrix Displacement Analysis", *Int. J. for Numerical Methods in Eng.*, **6**, 1973.
5. Timoshenko, S.: *Theory of Elasticity*. McGraw-Hill, 1934.
6. Callinan, R. J.: "User's Manual for DISMAL—A General Purpose Structural Analysis Program", ARL Structures and Materials Tech. Memo. 227, 1975.
7. Moore, D. W. G.: Program Information Sheet No. 87, University of W.A. Computer Centre, 1970.
8. Petersen, R.: *Stress Concentration Factors*. J. Wiley and Sons, 1974.

APPENDIX A

Determination of Fourier Coefficients

The applied loads are represented as:

$$\sigma_a(\theta) = \sigma_{a0}/2 + \sum_{n=1}^{Ns} \{\sigma_{an} \cos n\theta + \sigma_{an} \sin n\theta\} \tag{A.1}$$

$$\tau_a(\theta) = -\tau_{a0}/2 + \sum_{n=1}^{Ns} \{\tau_{an} \sin n\theta - \tau_{an} \cos n\theta\} \tag{A.2}$$

Where

$$\sigma_{an} = \frac{1}{\pi}\int_0^{2\pi} \sigma_a(\theta) \cos n\theta d\theta \tag{A.3}$$

$$\sigma_{an} = \frac{1}{\pi}\int_0^{2\pi} \sigma_a(\theta) \sin n\theta d\theta \tag{A.4}$$

$$\tau_{an} = \frac{1}{\pi}\int_0^{2\pi} \tau_a(\theta) \sin n\theta d\theta \tag{A.5}$$

$$\tau_{an} = -\frac{1}{\pi}\int_0^{2\pi} \tau_a(\theta) \cos n\theta d\theta \tag{A.6}$$

The Fourier coefficients σ_{an}, σ_{an}', τ_{an}, τ_{an} can be determined in three ways depending on the method of specifying the applied loading, $\sigma_a(\theta)$, $\tau_a(\theta)$.

(1) If the applied stress distributions, $\sigma_a(\theta)$ and $\tau_a(\theta)$ are trigonometric as $\sin n\theta$ or $\cos n\theta$, then the coefficients are known directly. Also if the distributions $\sigma_a(\theta)$ and $\tau_a(\theta)$ are known functions, such that the integrals of equations (A.3) to (A.6) can be easily evaluated analytically, then the coefficients can be evaluated external to the program and input to it.

(2) As a special case of known functions, if point loads are applied then $\sigma_a(\theta)$ and $\tau_a(\theta)$ are delta functions of the form:

$$\sigma_a(\theta) = \frac{P_{ai}}{r_0 b}\delta(\theta - \theta_i) \tag{A.7}$$

$$\tau_a(\theta) = \frac{S_{ai}}{r_0 b}\delta(\theta - \theta_i) \tag{A.8}$$

Where P_{ai} and S_{ai} are radial and shear loads applied at θ_i, r_0 is the hole radius, and b the element thickness. Then Equations (A.3) to (A.6) become:

$$\sigma_{an} = \frac{P_{ai}}{\pi r_0 b} \cos n\theta_i \tag{A.9}$$

$$\sigma_{an} = \frac{P_{ai}}{\pi r_0 b} \sin n\theta_i \tag{A.10}$$

$$\tau_{an} = \frac{S_{ai}}{\pi r_0 b} \sin n\theta_i \tag{A.11}$$

$$\tau_{an} = -\frac{S_{ai}}{\pi r_0 b} \cos n\theta_i \tag{A.12}$$

(3) If $\sigma_a(\theta)$ and $\tau_a(\theta)$ are complex or unknown functions, they can be input as ordinate values at N_p discrete values of θ. The points are equally spaced and labelled 0 - N_p - 1 where N_p is an even number. The distributions $\sigma_a(\theta)$ and $\tau_a(\theta)$ are then represented as Fourier series by taking the Discrete Fourier Transform of these points. The DFT is given by:

$$\sigma_a(\theta) = \frac{\sigma_{a0}}{2} + \sum_{n=1}^{\frac{1}{2}N_p - 1} \{\sigma_{an} \cos n\theta + \sigma_{an'} \sin n\theta\} + \frac{\sigma_{a\frac{1}{2}N_p}}{2} \cos\left\{\frac{N_p}{2}\theta\right\} \quad \text{(A.13)}$$

$$\tau_a(\theta) = \frac{\tau_{a0}}{2} + \sum_{n=1}^{\frac{1}{2}N_p - 1} \{\tau_{an} \cos n\theta + \tau_{an'} \sin n\theta\} + \frac{\tau_{a\frac{1}{2}N_p}}{2} \cos\left\{\frac{N_p}{2}\theta\right\} \quad \text{(A.14)}$$

Where

$$\sigma_{an} = \frac{2}{N_p} \sum_{m=1}^{N_p - 1} \sigma_a(\theta_m) \cos(2mn\pi/N_p) \quad \text{(A.15)}$$

$$\sigma_{an'} = \frac{2}{N_p} \sum_{m=1}^{N_p - 1} \sigma_a(\theta_m) \sin(2mn\pi/N_p) \quad \text{(A.16)}$$

$$\tau_{an} = \frac{2}{N_p} \sum_{m=0}^{N_p - 1} \tau_a(\theta_m) \cos(2mn\pi/N_p) \quad \text{(A.17)}$$

$$\tau_{an'} = \frac{2}{N_p} \sum_{m=1}^{N_p - 1} \tau_a(\theta_m) \sin(2mn\pi/N_p) \quad \text{(A.18)}$$

Equations (A.15) to (A.18) are numerical evaluations of equations (A.3) to (A.6). The coefficients σ_{an} , $\sigma_{an'}$, τ_{an} , $\tau_{an'}$ are evaluated using a DFT package program. The DFT can be put in the form of Equations (A.1) and (A.2) by using the following relationships.

$$\sigma_{an} = \sigma_{an} \quad \text{(A.19)}$$

$$\sigma_{an'} = \sigma_{an'} \quad \text{(A.20)}$$

$$\tau_{an} = \tau_{an} \quad \text{(A.21)}$$

$$\tau_{an'} = -\tau_{an'} \quad \text{(A.22)}$$

$$N_S = N_p/2 \quad \text{(A.23)}$$

$$\sigma_{aN_S} = 0{\cdot}5\sigma_{a\frac{1}{2}N_p} \quad \text{(A.24)}$$

$$\tau_{a'N_S} = -0{\cdot}5\tau_{a\frac{1}{2}N_p} \quad \text{(A.25)}$$

APPENDIX B

Input Data File

The input data file is entitled HIN and contains all parameters necessary to define the element geometry and material properties, the stress evaluation points, and the applied loading. The layout of the parameters in file HIN is given below.

HIN

r_0, r_1, b, f
N
$\gamma(1)$, $\gamma(2)$, . . . , $\gamma(N)$
E, ν
X_0, Y_0, X_1, Y_1
N_B
$\theta_B(1)$, $\theta_B(2)$, . . . , $\theta_B(N_B)$ {Omit if $N_B = 0$}
N_G
$r_G(1)$, $\theta_G(1)$, $r_G(2)$, $\theta_G(2)$, . . . , $r_G(N_G)$, $\theta_G(N_G)$ {Omit if $N_G = 0$}
[
P {= TRIG}
N_T
n, σ_{an}, σ_{an}, . . . , τ_{an}, τ_{an}
n, σ_{an}, . . . {etc. for N_T lines}
]
[
P {= POINT}
N_P, N_S
θ_i, P_{ai}, S_{ai}
θ_i, P_{ai}, . . . {etc. for N_P lines}
]
[
P {= NUMER}
M_1
$\sigma_a(1)$, $\sigma_a(2)$, $\sigma_a(3)$, . . . , $\sigma_a(N_{F0})$
$\tau_a(1)$, $\tau_a(2)$, $\tau_a(3)$, . . . , $\tau_a(N_{F0})$
]
P {= END}

The statements enclosed in curly brackets are comments and not part of the file. The file segments delineated by square brackets can be placed in any order and any segment type can be repeated or omitted. For no applied loading, all three segments should be omitted. All quantities in the file are in list directed format. Where practicable, the parameter symbols in the above file layout correspond with symbols used in the main body of this report, rather than with the variable names used in the program. For clarity, all symbols are defined in Table B1 and their limitations prescribed. All parameters referred to in Table B1 as "numbers" are integers. Other unspecified parameters are real numbers. All angles are input in degrees. Other quantities are input in any self-consistent set of units. The program was developed for anticlockwise node numbering and its successful operation for clockwise numbering has not been confirmed. For applied loading, the sign convention is positive for inward radial loads and anticlockwise shear loads. Naturally, all limits specified in Table B1 are in addition to inherent sensibility limits, e.g. it would be nonsense to specify a negative element thickness, b.

As an example, the data file HIN for a doubly symmetric loaded hole element with 10 nodes is listed below. The hole radius is 2·0 m, the element circumscribing radius is 4·0 m and the element thickness 0·002 m. Stresses are to be evaluated at three hole boundary points only. Applied loading consists of a point load superimposed on a distributed load.

HIN

```
2·0, 4·0, 0·002, 0·25
10
0·0, 10·0, 20·0, 30·0, 40·0, 50·0, 60·0, 70·0, 80·0, 90·0
7·10E07, 0·3
0·0, 0·0, 1·0, 0·0
3
5·0, 15·0, 25·0
0
 POINT
1, 8
45·0, 1000·0, 0·0
 NUMER
4
1·0E05, 1·2E05, 1·4E05, 1·3E05, 1·1E05
0·0, 1·5E05, 1·6E05, 1·5E05, 0·0
 END
```

TABLE B1

Input Parameter Definitions

Symbol	Definition	Limits
r_0	Hole radius	$r_0 > 0$
r_1	Element circumscribing radius	$r_1 > r_0$ and $1{\cdot}5 < r_1/r_0 < 3{\cdot}0$ for best accuracy
b	Element thickness	Validity of plane stress assumption
f	Element fraction of a full circle	$= 0{\cdot}25$ for doubly symmetric $= 0{\cdot}5$ for singly symmetric $= 1{\cdot}0$ for unsymmetric
N	Number of nodes	$3 \leqslant N \leqslant 10$
$\gamma(i)$	Angular co-ordinate of node i	$\gamma(i) >$ all $\gamma(j)$, for $j < i$ $\gamma(N) - \gamma(1) = 360f$, for $f \neq 1{\cdot}0$ $< 360f$, for $f = 1{\cdot}0$
E	Young's modulus	None
ν	Poisson's ratio	None
X_0, Y_0	Global cartesian co-ordinate of the hole centre	None
X_1, Y_1	Global cartesian co-ordinate of node 1	None
N_B	Number of hole boundary points for stress evaluation	$N + N_B + 3N_G \leqslant 30$
$\theta_B(i)$	Angular co-ordinate of boundary stress evaluation point i	None
N_G	Number of general points for stress evaluation	$N + N_B + 3N_G \leqslant 30$
$r_G(i)$, $\theta_G(i)$	Local polar co-ordinates of general stress evaluation point i	None
P	A flag to specify the type of loading	TRIG, POINT, NUMER, END
N_T	Number of frequencies for which Fourier coefficients are input	None
n	Frequency parameter	Integer, $0 \leqslant n \leqslant 16$
σ_{an}, σ_{an}	Coefficients of $\cos n\theta$ and $\sin n\theta$ for applied normal stress	These functions are referenced to node 1 as $\theta = 0$
τ_{an}, τ_{an}	Coefficients of $\cos n\theta$ and $\sin n\theta$ for applied shear stress	These functions are referenced to node 1 as $\theta = 0$
N_P	Number of positions at which point loads are applied	None
N_S	Cut-off frequency for Fourier representation of point loads	Integer, $0 \leqslant N_S \leqslant 16$
θ_i	Angular co-ordinate of point load position i	None
P_{ai}, S_{ai}	Radial and shear point load components at position i	None
M_1	Parameter defining the number of input ordinate values, N_{F0}	Even integer < 8, 10, 12 for $f = 0{\cdot}25$, $0{\cdot}5$, $1{\cdot}0$
N_{F0}	Number of input ordinate values	$N_{F0} = 2^{M_1/2} + 1$
$\sigma_a(i)$, $\tau_a(i)$	The ith normal and shear stress ordinate values	Ordinate values are for equally spaced points around hole boundary. For $f = 0{\cdot}25$, $0{\cdot}5$, points 1 and N_{F0} lie at nodes 1 and N respectively, and $\tau_a(1) = \tau_a(N_{F0}) = 0$. For $f = 1{\cdot}0$, points 1 and N_{F0} lie at node 1 and $\sigma_a(1) = \sigma_a(N_{F0})$ and $\tau_a(1) = \tau_a(N_{F0})$

APPENDIX C

Operating Instructions

The step-by-step operations for using the loaded hole element program, HOLE, in conjunction with the general finite element analysis suite of programs, DISMAL, are listed below.

(1) Draw up the mesh for the structure, including any loaded hole elements, and define the applied loads.

(2) Prepare the data file, DATA, for DISMAL (see Ref. 6), excluding the applied loading data at this stage. Loaded hole elements are specified in DATA as special elements (see Ref. 6).

(3) For each loaded hole element (in the order of specification in DATA) prepare a data file, HIN (see Appendix B), run the program HOLE, and obtain a listing of CHECK.LST.

(4) Complete the applied loading section in DATA including the equivalent nodal forces obtained from the listings of CHECK.LST.

(5) Run the DISMAL programs (see Ref. 6).

(6) Obtain the stresses for the loaded hole elements from the DISMAL output file PRINT3.LST. These stresses will be output in the order of: tangential stress for nodal point projections followed by specified boundary stress evaluation points; then followed by sets of radial, tangential and shear stress for general stress evaluation points. Add these stresses to the corresponding initial stresses obtained from the listings of CHECK.LST.

The above instructions apply to the case where only one load case is specified in DATA. If more than one load case is to be specified, involving different loading on the holes, it will be necessary to establish equivalent nodal forces and initial stresses by preliminary runs of HOLE, and then establish the correctly structured files DATA.EXT and SPIT by an appropriate sequence of runs of HOLE. The loaded hole element can be used in conjunction with other special elements, providing the correct appending of files DATA.EXT and SPIT is monitored.

DISTRIBUTION

AUSTRALIA

DEPARTMENT OF DEFENCE AND DEPARTMENT OF DEFENCE SUPPORT

Central Office

Chief Defence Scientist
Deputy Chief Defence Scientist
Superintendent, Science and Technology Programmes
Controller, Projects and Analytical Studies Division
(1 copy)
Defence Science Representative (UK) (Doc Data Sheet only)
Counsellor, Defence Science (USA) (Doc Data Sheet only)
Defence Central Library
Document Exchange Centre, DISB (17 copies)
Joint Intelligence Organisation
Librarian, H Block, Victoria Barracks, Melbourne
Director-General Army Development (NSO) (4 copies)

Aeronautical Research Laboratories

Chief Superintendent
Library
Superintendent Structures
Divisional File Structures
Author: K. C. Watters
R. Jones
R. J. Callinan
T. C. Ryall

Materials Research Laboratories

Chief Superintendent Library

Defence Research Centre

Library

Central Studies Establishment

Information Centre

Navy Office

Navy Scientific Adviser
RAN Aircraft Maintenance and Flight Trials Unit
Directorate of Naval Aircraft Engineering
Superintendent, Aircraft Maintenance and Repair
Directorate of Naval Ship Design

Army Office

Army Scientific Adviser
Engineering Development Establishment, Library
Royal Military College Library
US Army Research, Development and Standardisation Group

Air Force Office
- Aircraft Research and Development Unit
  - Scientific Flight Group
  - Library
- Air Force Scientific Adviser
- Technical Division Library
- Director-General Aircraft Engineering—Air Force
- HQ Support Command (SENGSO)
- RAAF Academy, Point Cook

Government Aircraft Factories
- Manager
- Library

DEPARTMENT OF AVIATION
- Library
- Flying Operations and Airworthiness Division

STATUTORY AND STATE AUTHORITIES AND INDUSTRY
- Trans-Australia Airlines, Library
- Qantas Airways Limited
- SEC of Victoria, Herman Research Laboratory, Library
- Ansett Airlines of Australia, Library
- BHP, Melbourne Research Laboratories
- Commonwealth Aircraft Corporation, Library
- Hawker de Havilland Aust. Pty. Ltd., Bankstown, Library
- Rolls-Royce of Australia Pty. Ltd., Mr. C. G. A. Bailey

UNIVERSITIES AND COLLEGES

Adelaide	Barr Smith Library
	Professor of Mechanical Engineering
Flinders	Library
La Trobe	Library
Melbourne	Engineering Library
Monash	Hargrave Library
Newcastle	Library
Sydney	Engineering Library
New South Wales	Professor R. A. A. Bryant, Mechanical Engineering
	Physical Science Library
	Associate Professor R. W. Traill-Nash, Civil Engineering
Queensland	Library
Tasmania	Engineering Library
Western Australia	Library
	Associate Professor J. A. Cole, Mechanical Engineering
RMIT	Library
	Dr. H. Kowalski, Mechanical and Production Engineering

CANADA
- CAARC Co-ordinator, Structures
- International Civil Aviation Organization, Library
- NRC Aeronautical and Mechanical Engineering Library

Universities and Colleges

Toronto	Institute of Aerospace Studies

FRANCE
ONERA, Library

GERMANY
Fachinformationszentrum: Energie, Physic, Mathematik GmbH

INDIA
CAARC Co-ordinator Structures
Defence Ministry, Aero Development Establishment, Library
Gas Turbine Research Establishment, Director
Hindustan Aeronautics Ltd., Library
National Aeronautical Laboratory, Information Centre

ISRAEL
Technion-Israel Institute of Technology, Professor J. Singer

JAPAN
Institute of Space and Astronautical Science, Library

NETHERLANDS
National Aerospace Laboratory (NLR), Library

NEW ZEALAND
RNZAF, Vice-Consul (Defence Liaison)
Transport Ministry, Airworthiness Branch, Library
Universities
Canterbury Library
Professor D. Stevenson, Mechanical Engineering

SWEDEN
Aeronautical Research Institute, Library

SWITZERLAND
Armament Technology and Procurement Group
F + W (Swiss Federal Aircraft Factory)

UNITED KINGDOM
CAARC, Secretary (NPL)
Royal Aircraft Establishment, Bedford, Library
Admiralty Marine Technology Establishment, St. Leonard's Hill, Superintendent
National Gas Turbine Establishment, Pyestock North, Director
National Engineering Laboratory, Library
British Library, Lending Division
CAARC Co-ordinator, Structures
Aircraft Research Association, Library
British Ship Research Association
GEC Gas Turbines Ltd., Managing Director
Motor Industry Research Association, Director
Rolls-Royce Ltd., Aero Division, Bristol, Library
British Aerospace
Kingston-upon-Thames, Library
Hatfield-Chester Division, Library
British Hovercraft Corporation Ltd., Library
Short Brothers Ltd., Technical Library

Universities and Colleges

Bristol	Engineering Library
Cambridge	Library, Engineering Department
	Whittle Library
London	Professor G. J. Hancock, Aero Engineering
Manchester	Professor, Applied Mathematics
Nottingham	Science Library
Southampton	Library
Strathclyde	Library
Cranfield Institute of Technology	Library
Imperial College	Aeronautics Library

UNITED STATES OF AMERICA

NASA Scientific and Technical Information Facility
The John Crerar Library
Allis Chalmers Corporation, Library
Boeing Company, Mr. R. Watson
Kentex Research Library
United Technologies Corporation, Library
Lockheed California Company
Lockheed Missiles and Space Company
Lockheed—Georgia
McDonnell Aircraft Company, Library

Universities and Colleges

Johns Hopkins	Professor S. Corrsin, Engineering
Princeton	Professor G. L. Mellor, Mechanics
Massachusetts Inst. of Technology	MIT Libraries

Spares (10 copies)

Total, 152 copies

Department of Defence

DOCUMENT CONTROL DATA

1. a. AR No.	1. b. Establishment No.	2. Document Date	3. Task No.
AR-002-895	ARL-STRUC-REPORT-392	June, 1982	DST 82 010

4. Title	5. Security	6. No. Pages
SPECIAL FINITE ELEMENTS FOR SHEETS WITH LOADED CIRCULAR HOLES	a. document: Unclassified b. title: U c. abstract: U	20 7. No. Refs: 8

8. Author(s)	9. Downgrading Instructions
K. C. Watters	—

10. Corporate Author and Address	11. Authority (*as appropriate*)
Aeronautical Research Laboratories, P.O. Box 4331, Melbourne, Vic. 3001	a. *Sponsor* c. Downgrading b. Security d. Approval a) DSTO

12. Secondary Distribution (*of this document*)
Approved for public release

Overseas enquirers outside stated limitations should be referred through ASDIS, Defence Information Services, Branch, Department of Defence, Campbell Park, CANBERRA, ACT 2601.

13. a. This document may be ANNOUNCED in catalogues and awareness services available to . . .
No limitations

13. b. Citation for other purposes (*i.e. casual announcement*) may be (*select*) unrestricted (*or*) as for 13 a.

14. Descriptors	15. COSATI Group
Continuum mechanics	
Loads (forces)	2011
Stress concentration	1201
Finite element method	
Hybrid elements	
Holes	

16. Abstract

This paper describes a special hybrid finite element to represent a loaded hole in a sheet. The shape functions of the element satisfy stress equilibrium and strain compatibility throughout the element, and the applied loading boundary conditions. The applied loading is represented by a finite Fourier series, and the coefficients of the element shape functions are matched with the Fourier coefficients. A computer program has been written to generate the element stiffness and stress recovery matrices. The program also produces equivalent nodal forces and initial stresses related to the applied loading. Accurate results have been obtained from several example analyses.

This page is to be used to record information which is required by the Establishment for its own use but which will not be added to the DISTIS data base unless specifically requested.

16. Abstract (*Contd*)

17. Imprint

Aeronautical Research Laboratories, Melbourne

18. Document Series and Number	19. Cost Code	20. Type of Report and Period Covered
Structures Note 392	21 7041	—

21. Computer Programs Used

HOLE (FORTRAN)

22. Establishment File Ref(s)

END

DATE
FILMED

4-83

DTIC